Journal of Alloys and Compounds 509 (2011) 8478–8482

Contents lists available at ScienceDirect

Journal of Alloys and Compounds

journal homepage: www.elsevier.com/locate/jallcom

Growth and characterization of tetragonal structure modification of β-$Gd_2Si_2O_7$:Ce

V. Baumer[a], I. Gerasymov[b], O. Sidletskiy[b,*], O. Voloshina[b], S. Neicheva[b]

[a] State Scientific Institution "Institute for Single Crystals" National Academy of Sciences of Ukraine, 60, Lenin Ave., Kharkiv, 61001, Ukraine
[b] Institute for Scintillation Materials National Academy of Sciences of Ukraine, 60, Lenin Ave., Kharkiv, 61001, Ukraine

ARTICLE INFO

Article history:
Received 27 December 2010
Received in revised form 1 June 2011
Accepted 6 June 2011
Available online 12 June 2011

Keywords:
Scintillation materials
β-$Gd_2Si_2O_7$
Crystal structure
Luminescence

ABSTRACT

Growth procedure, crystal structure, and luminescent properties of tetragonal β-$Gd_2Si_2O_7$:0.5 at.% Ce (a = 6.65740(10) Å, c = 24.2715(3) Å, sp.gr. $P4_3$) are studied. Tetragonal modification of this compound is obtained for the first time. Essentially it is isostructural to β-$Sm_2Si_2O_7$ and some other known disilicates (Ca, La, Ce, Pr, Nd). Obtained samples demonstrate high luminescence yield under X-rays and fast decay.

1. Introduction

Radiation monitoring, high-energy physics, medical diagnostics devices, well logging, etc. are the basic domains of scintillation materials application. At present, rare earth silicates RE_2SiO_5 and aluminates $RE_3Al_5O_{12}$, $REAlO_3$ (RE = Y, Gd, Lu) activated with Ce^{3+} or Pr^{3+} are widely applied in many fields [1]. Search for new materials with improved scintillation characteristics is of big importance. Cerium-doped lutetium scandium orthoborate $(Lu_{1-x}Sc_x)BO_3$ [2], gadolinium silicate $Gd_{9.33}(SiO_4)_6O_2$ (GSAP:Ce) [3], Ce, Na-codoped lutetium silicate Lu_2SiO_5 [4] are the recent examples of new scintillation materials based on complex oxides. Ce-doped rare earth pyrosilicates (disilicates) $RE_2Si_2O_7$ are among the most promising new scintillators. They possess lower crystallization temperatures and lower cost of starting components in comparison to those for oxyorthosilicates. Pyrosilicates demonstrate attractive scintillation characteristics at monitoring of γ-radiation [5,6] and thermal neutrons [7], in particular, outstanding light yield stability at elevated temperatures. Recently, growth procedure, and scintillation and luminescence characteristics of Ce-doped $Gd_2Si_2O_7$ (GPS) [8] and $Y_2Si_2O_7$ [9], Pr^{3+}-doped $Lu_2Si_2O_7$ (LPS) [10,11] and $Gd_2Si_2O_7$ [12], and Eu-doped $Y_2Si_2O_7$ and $La_2Si_2O_7$ [13] were reported.

Rare earth pyrosilicates demonstrate big variety of crystalline structures depending on rare earth cation radius and conditions of obtaining. Hence, process of GPS:Ce crystal growth, as well as other pyrosilicates with RE cation size more than 0,87 Å, is complicated because of incongruent melting of RE_2O_3–SiO_2 compositions with molecular ratio 1:2. In accordance with the phase diagram (Fig. 1), with the cooling of the melt, $2Gd_2O_3{\cdot}3SiO_2$ crystals precipitate from the melt when the temperature reaches the liquidus curve for the initial composition $Gd_2O_3{\cdot}2SiO_2$. There are two known methods to overcome this problem. The first one was demonstrated in [8,15,16] where GPS:Ce or GPS:Pr single crystals were obtained by the Floating Zone and Czochralski methods from stoichiometric melt with heavy (up to 25 at.%) Ce^{3+} and Pr^{3+} doping, correspondingly. It was assumed [15] that the heavy doping changes phase diagram and enables direct crystallization of single crystalline samples from the melt. Depending on Ce concentration, orthorhombic, triclinic, and monoclinic modifications of $Gd_2Si_2O_7$:Ce can be obtained [16]. However, high Ce concentration in this method evidently should lead to concentration quenching and drop of light yield. The second approach is to crystallize GPS, or mixed pyrosilicate (LaGPS) from melt-solution with the self-flux of SiO_2 (silicon oxide concentration 71–73.6 mol.%) [17,18]. This method allows one to grow crystals with low Ce concentrations and higher luminescence intensities [19]. The one of the highest luminescence yields in comparison with other structures (orthorhombic, triclinic) was demonstrated on tetragonal mixed pyrosilicate $Gd_{2x}La_{2-2x}Si_2O_7$:Ce [19]. Therefore, search for other compositions with this type of structure is a topic of scientific and practical interest. This work describes the growth procedure and characterization of Ce-doped tetragonal gadolinium pyrosilicate (β-$Gd_2Si_2O_7$) without La addition. This crystalline structure has never been observed before with GPS:Ce.

* Corresponding author. Tel.: +380 57 341 04 42; fax: +380 57 340 44 74.
E-mail address: sidletskiy@isma.kharkov.ua (O. Sidletskiy).

0925-8388/$ – see front matter © 2011 Elsevier B.V. All rights reserved.
doi:10.1016/j.jallcom.2011.06.016

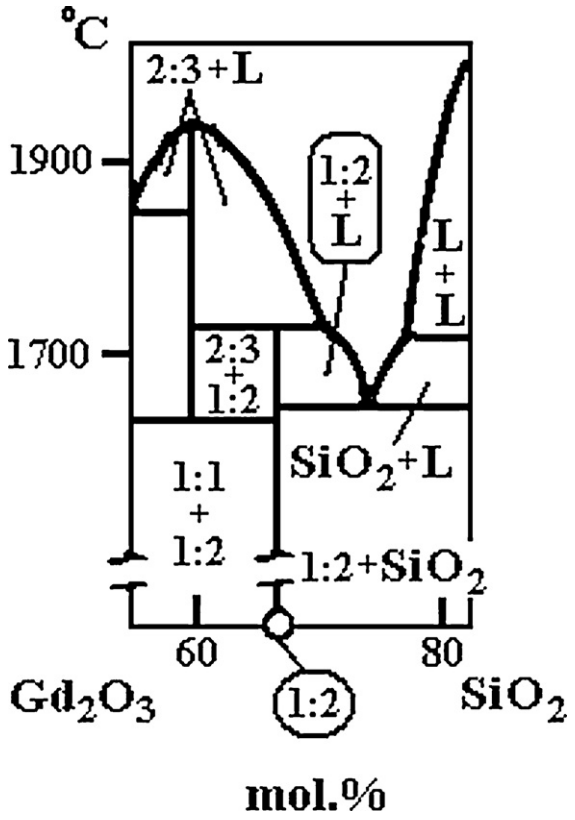

Fig. 1. Fragment of the Gd_2O_3–SiO_2 phase diagram taken from [14].

2. Experimental

2.1. Obtaining of crystalline samples

Raw material for crystal growth was prepared by solid-phase synthesis. The starting components were gadolinium oxide Gd_2O_3 (4 N), silicon oxide SiO_2 (5 N), cerium oxide CeO_2 (4 N) (Stanford Materials). They were mixed in composition according to the molar ratio $26.5Gd_2O_3$:$0.5CeO_2$:$73SiO_2$, that is, the composition corresponded to the near-peritectic concentration (see Fig. 1). Mixing was carried out in a rod mill made of acrylic plastic. Starting materials were calcined at 600 °C to remove absorbed moisture and CO_2, then, they were heated up to 1700 °C to synthesize the pyrosilicate phase by the analogy with [20].

Gadolinium pyrosilicate crystals were obtained by melting of around 100 g of the raw material in Ir crucible with the diameter 35 mm and height 12 mm and its consecutive crystallization on iridium wire. The crucible was placed in Ar atmosphere (pressure around 10^5 Pa) in RF-heating furnace. The powder was completely melted at temperature around 1750 °C. Construction of crystallizer provided high temperature gradient (>100 °/cm) above the melt. After choice of required crystallization conditions, the wire rotating with the rate 10 rpm was pulled up from melt at the 1 mm/h rate. After cutoff from melt the crystals were cooled to room temperature for 30 h.

2.2. Determination of crystal structure

Crystal structure of obtained crystalline samples were determined using an X-ray automated single crystal diffractometer ((Xcalibur-3)) (Oxford Diffraction Ltd.) equipped with ((Sapphire-3)) CCD-detector and graphite monochromator, and X-ray automated powder diffractometer ((Siemens D500)) (CuKα radiation, curved graphite monochromator on a counter arm, $5° \le 2\theta \le 120°$, $\Delta 2\theta = 0.02°$, dwell time of 8 s per point). Data processing was carried out using a SHELX-97 program package [21] and FullProf-2006 program [22].

2.3. Study of luminescent characteristics

Luminescent and kinetic characteristics of the obtained crystals were measured in comparison with orthorhombic $Gd_2Si_2O_7$:10 at.% Ce [19]. All the ingots were crushed and pressed under 2×10^7 Pa pressure into pellets with 2 mm thickness and 10 mm diameter. Excitation and luminescence spectra at room temperature in the 230–800 nm range and decay curves at photo excitation were determined with a combined fluorescent lifetime and steady-state spectrometer FLS 920 (Edinburgh Instruments). Xe lamp was used for steady-state measurements and nanosecond hydrogen operated flashlamp was used for decay time measurements. X-ray luminescence was measured at excitation by X-ray tube with copper anode (braking radiation with the 30 keV energy).

Table 1
Crystal data and structure refinement for β-$Gd_2Si_2O_7$:0.5 at.% Ce.

Empirical formula	$Gd_2\ O_7\ Si_2$
M_r	482.68
Temperature	293(2) K
Wavelength MoKα	0.71073 Å
Crystal system, space group	Tetragonal, $P4_3$
Unit cell dimensions	$a = 6.65740(10)$, $c = 24.2715(3)$ Å
V_{cell}	1075.74(3) Å
Z, ρ_{calc}	8, 5.961 Mg/m^3
μ(MoKα)	24.874 mm^{-1}
$F(0\,0\,0)$	1696
Crystal size	$0.15 \times 0.01 \times 0.01$ mm
θ range for data collection	3.06–45.72°.
Index ranges	$-13 \le h \le 13$, $-12 \le k \le 11$, $-48 \le l \le 48$
Reflections collected/unique	23930/8842 ($R_{int} = 0.044$)
Completeness to $2\theta = 45.00°$	99.6%
Transmission T_{max}/T_{min}	0.7890 and 0.1180
Refinement method	Full-matrix least-squares on F^2
Data/parameters	8842/204
Goodness-of-fit on F^2	0.974
Final R indices [I > 2σ(I)]	$R_1 = 0.0327$, w$R_2 = 0.0320$
R indices (all data)	$R_1 = 0.0492$, w$R_2 = 0.0336$
Absolute structure parameter	−0.008(7)
Extinction coefficient κ	0.000546(14)
$\Delta\rho_{max}/\Delta\rho_{min}$	2.029/−2.157 e × Å^{-3}

3. Results and discussion

3.1. Growth procedure and structure of β-$Gd_2Si_2O_7$:0.5 at.% Ce

In accordance with [14,20], tetragonal modification of disilicates exists for RE cations with radii greater than 0.947 Å (from La to Eu). The average RE cation radius of mixed tetragonal gadolinium–lanthanum pyrosilicate ($Gd_{2x}La_{2-2x}Si_2O_7$:Ce) obtained in [19] is the same as for $Eu_2Si_2O_7$ (0.947 Å), therefore, it is situated in the specified range. As it was suggested before [17,23], pure gadolinium pyrosilicate (cation radius of Gd^{3+} is 0.938 Å) can be obtained only in orthorhombic or triclinic modifications. Small amount of cerium in $Gd_2Si_2O_7$:0.5 at.% Ce crystals grown in the present work cannot significantly affect the average RE cation radius, therefore, it is the same as for Gd^{3+} (0.938 Å). Hence its composition is out of the known range of tetragonal phase existence. We suggest that growth of GPS:Ce crystals of low-temperature tetragonal modification became possible due to high temperature gradient near the crystallization interface and the prolonged post-growth cooling. Obtained crystals were colorless and transparent; however, they contained a large number of cracks owing to the seeding onto iridium wire and high thermal gradient over the melt. The possible orthorhombic-tetragonal or orthorhombic-triclinic-tetragonal polymorph transitions in crystal during the cooling process also should not be excluded from the consideration.

Main crystal data and bond lengths obtained from XRD measurements are summarized in Tables 1 and 2. Thermal ellipsoids and labeling scheme for basis atoms are shown in Fig. 2. Crystal packing drawn with "Ball & Stick" program [24] is shown in Fig. 2. Figs. 2 and 3 were constructed on the basis of the measured parameters. Rietveld refinement was carried out using the structure data obtained in X-ray single crystal study and shows (Fig. 4) that all lines correspond to single phase.

In this structure the unit cell contains four gadolinium atoms and two disilicate polyhedrons as a basis (Fig. 2). Oxygen arrangement is different for Gd atoms in the structure. Gd(1) and Gd(3) atoms are eight coordinated, Gd(2) atom is nine coordinated, and Gd(4)

Table 2
Selected bond lengths (Å) for β-$Gd_2Si_2O_7$:0.5 at.% Ce and symmetry transformations used to generate equivalent atoms. Standard deviations are given in parentheses.

Gd(1)-O(6)#1	2.309(2)	Gd(2)-O(4)#5	2.808(3)	Si(1)-O(3)	1.594(2)
Gd(1)-O(13)#2	2.342(2)	Gd(3)-O(6)#1	2.368(2)	Si(1)-O(1)	1.609(2)
Gd(1)-O(7)	2.377(2)	Gd(3)-O(14)#7	2.368(2)	Si(1)-O(4)	1.639(2)
Gd(1)-O(12)	2.438(2)	Gd(3)-O(1)	2.369(2)	Si(1)-O(2)	1.642(2)
Gd(1)-O(8)#3	2.503(2)	Gd(3)-O(8)#2	2.383(2)	Si(2)-O(6)	1.596(2)
Gd(1)-O(3)#4	2.533(2)	Gd(3)-O(9)	2.385(2)	Si(2)-O(5)	1.598(2)
Gd(1)-O(2)#4	2.556(2)	Gd(3)-O(2)#1	2.428(2)	Si(2)-O(7)	1.600(2)
Gd(1)-O(1)	2.754(2)	Gd(3)-O(11)#2	2.600(2)	Si(2)-O(4)	1.667(2)
Gd(2)-O(5)#5	2.321(2)	Gd(3)-O(4)#1	2.895(2)	Si(3)-O(10)	1.611(2)
Gd(2)-O(10)#6	2.3795(19)	Gd(4)-O(5)#8	2.247(2)	Si(3)-O(9)	1.614(2)
Gd(2)-O(7)	2.383(2)	Gd(4)-O(10)#6	2.291(2)	Si(3)-O(8)	1.623(2)
Gd(2)-O(12)	2.448(2)	Gd(4)-O(3)#5	2.302(2)	Si(3)-O(11)	1.649(2)
Gd(2)-O(9)#3	2.4748(18)	Gd(4)-O(12)	2.3672(19)	Si(4)-O(13)	1.585(3)
Gd(2)-O(14)#6	2.486(2)	Gd(4)-O(1)	2.395(2)	Si(4)-O(14)	1.628(2)
Gd(2)-O(13)	2.743(2)	Gd(4)-O(9)	2.540(2)	Si(4)-O(12)	1.630(2)
Gd(2)-O(8)#3	2.759(2)	Gd(4)-O(2)	2.619(2)	Si(4)-O(11)	1.675(2)

Symmetry transformations used to generate equivalent atoms

#1	$x,y+1,z$	#3	$y-1,-x,z+1/4$	#5	$x-1,y,z$	#7	$-y+1,x+1,z-1/4$
#2	$x+1,y,z$	#4	$y,-x+1,z+1/4$	#6	$x,y-1,z$	#8	$-y,x,z-1/4$

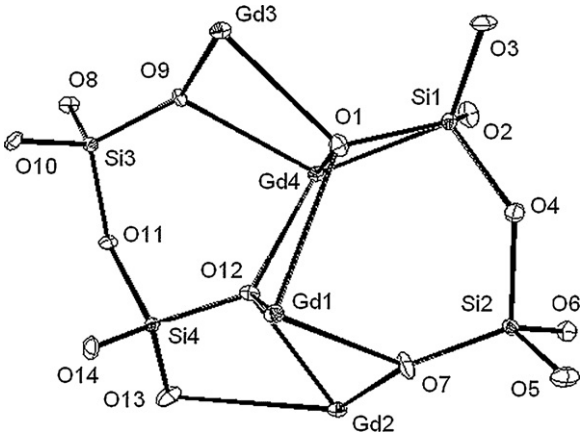

Fig. 2. ORTEP drawing (50% probability ellipsoids) and atom labeling scheme for β-$Gd_2Si_2O_7$:0.5 at.% Ce.

is seven coordinated. Gadolinium polyhedra form helix-like chains along [0 0 1] direction in the unit cell. Neighbor polyhedra in the chain are joined via common edges, and neighbor chains are sewn via common edges with silicon tetrahedra or common vertices with Gd polyhedra. Essentially observed β-$Gd_2Si_2O_7$:0.5 at.% Ce modification is isostructural to β-$Sm_2Si_2O_7$ [25] and other rare earth or calcium pyrosilicates [26] reported for larger RE^{3+} cations to within enantiomorph fixing (*e.g.* for β-$Sm_2Si_2O_7$ $a = 6.695$, $c = 24.40$ Å, sp.gr. $P4_1$ [23]). Samarium pyrosilicate is considered to be a low temperature modification, while the rest exist in certain temperature ranges or formed at high pressures. It should be noted that β-$Gd_2Si_2O_7$:0.5 at.% Ce structure stands out in compare to orthorhombic $Gd_2Si_2O_7$ from the point of possible Gd substitution by other ions. Rare earth cations in this lattice have different coordination numbers, while in orthorhombic α-modification the coordination number of the two basis atoms equals 7 impeding an isomorphic incorporation of rare earth cations with bigger ionic radius into this structure.

3.2. Luminescence characteristics

Normalized X-ray luminescence spectrum of tetragonal β-$Gd_2Si_2O_7$:0.5 at.% Ce is presented in Fig. 5. Spectra of orthorhombic $Gd_2Si_2O_7$:10 at.% Ce and previously grown tetragonal

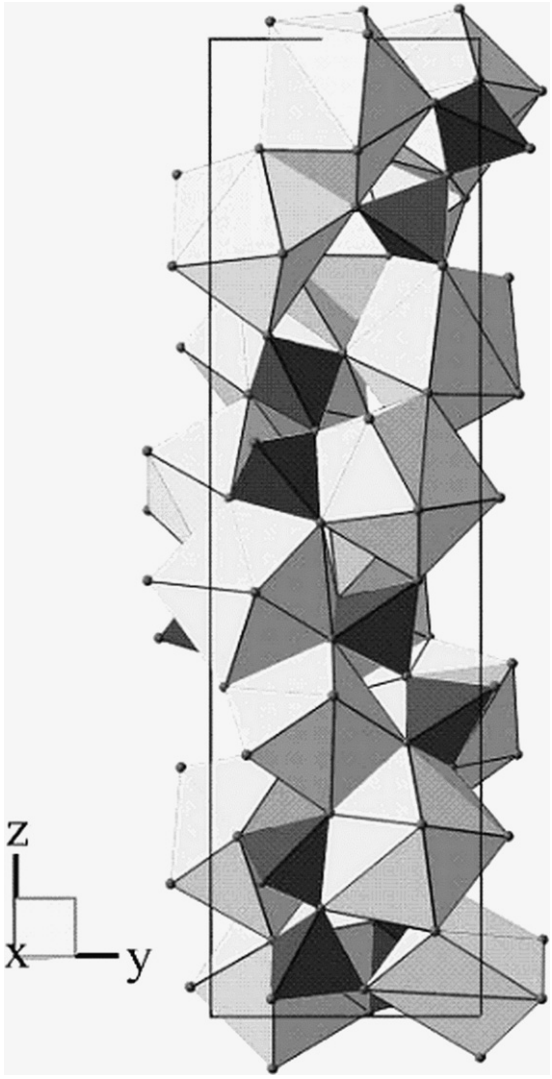

Fig. 3. Polyhedral representation of β-$Gd_2Si_2O_7$:0.5 at.% Ce structure. Space group-tetragonal, $P4_3$. Lattice parameters: $a = 6.65740(10)$ Å, $c = 24.2715(3)$ Å.

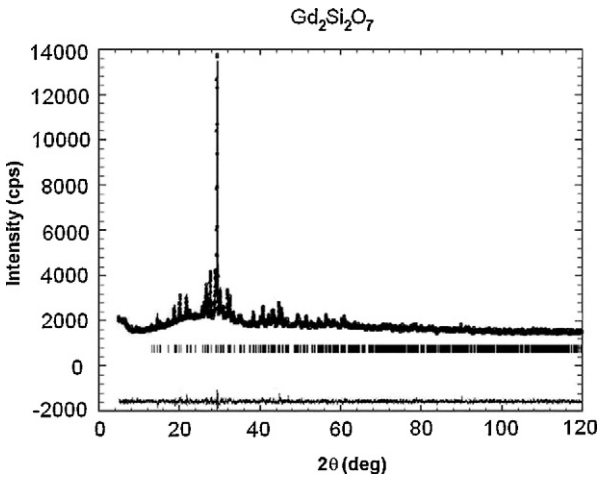

Fig. 4. Results of Rietveld refinement for β-$Gd_2Si_2O_7$:0.5 at.% Ce.

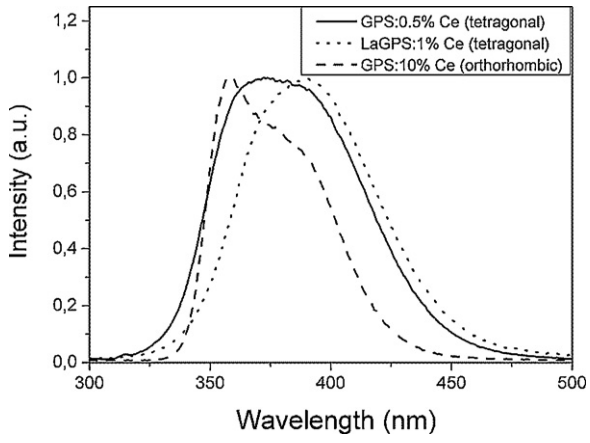

Fig. 5. Normalized X-ray luminescence spectra of tetragonal (β-$Gd_2Si_2O_7$:0.5 at.% Ce), tetragonal (β-$Gd_{1.8}La_{0.2}Si_2O_7$:1 at.% Ce), and orthorhombic ($Gd_2Si_2O_7$:10 at.% Ce) samples.

β-$Gd_{1.8}La_{0.2}Si_2O_7$:1 at.% Ce single crystals [19] are added for comparison. It should be noted that emission spectra of tetragonal β-$Gd_2Si_2O_7$:Ce is wider and more intense than those for orthorhombic modification. Integral intensity of β-$Gd_2Si_2O_7$:Ce luminescence is by 2.7 times higher than that for orthorhombic modification and comparable with β-$Gd_{1.8}La_{0.2}Si_2O_7$:1 at.% Ce crystal.

The ionic radius of Ce^{3+} ion is bigger (1.02 Å) than that for Gd^{3+} (0.938 Å), therefore one can conclude that Ce^{3+} ions should preferably occupy the largest 9-coordinated position (average Gd–O distance is 2.534 Å) and, then, 8- and 7-coordinated sites with Gd–O distances 2.477, 2.475, and 2.394 Å, respectively, see Table 2. Probably, the wide X-ray luminescence spectrum of β-$Gd_2Si_2O_7$:Ce is the result of superposition of peaks corresponding to different activator centers. More deep studies of concentration and temperature quenching of luminescence of Ce^{3+} in different coordination are necessary to describe so big difference in luminescence intensity between orthorhombic and tetragonal samples. It can be attributed both to peculiarities of tetragonal phase, and lower Ce concentration in tetragonal samples.

Photoluminescence measurements allow to distinguish emission characteristics of Ce^{3+} centers in β-$Gd_2Si_2O_7$:Ce (Fig. 6) though the emission and excitation bands of Ce centers are significantly overlap. Nevertheless, one can see four distinct excitation spectra. A set of bands in the 240–350 nm region and narrow peaks around 272 nm are observed in the excitation spectrum of β-$Gd_2Si_2O_7$:Ce. Narrow peaks are ascribed to transitions from ground state $^8S_{7/2}$ to the excited ^6I_j multiplets in Gd^{3+} ions. Wide bands obviously correspond to 4f–5d transitions in Ce^{3+} ions. The position of 4f–5d bands significantly depends on local site symmetry, so one can conclude that 4 types of excitation curves correspond to Ce ions occupying four different position in the lattice Fig. 7.

Photoluminescence decay measured at the intrinsic excitation is monoexponential with the decay time $\tau = 28$ ns (Fig. 7). All types of the luminescence centers in β-$Gd_2Si_2O_7$:Ce demonstrate similar decay profiles with the same time constant. This value is characteristic for Ce^{3+} ions and similar to those obtained for other Ce-doped disilicates (25–35 ns) [5,6,19].

This set of characteristics demonstrates a potential for practical application of β-$Gd_2Si_2O_7$:Ce. Obtaining of bulk and uncracked

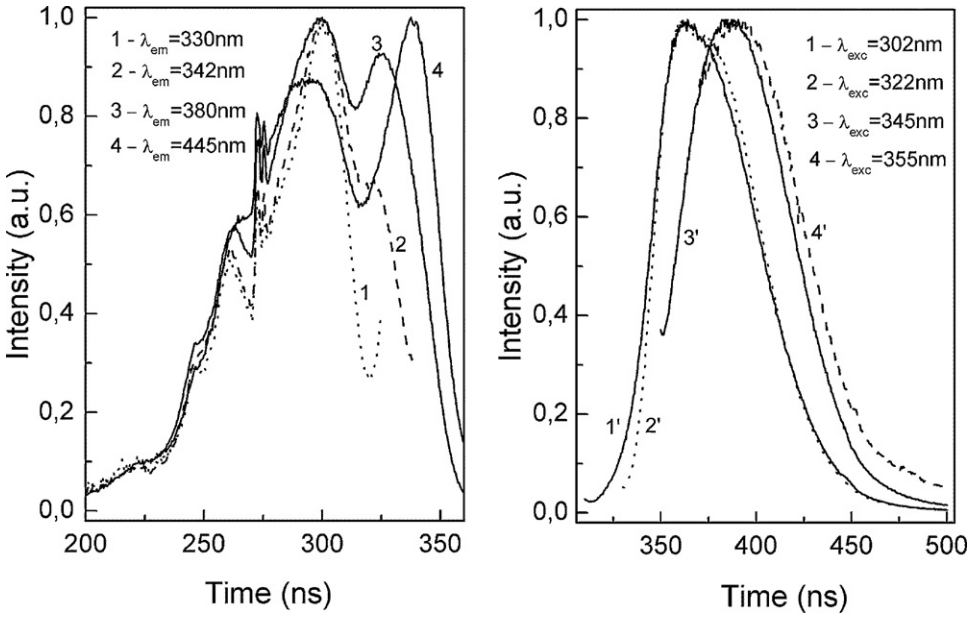

Fig. 6. Excitation (left) and emission (right) spectra of β-$Gd_2Si_2O_7$:0.5 at.% Ce.

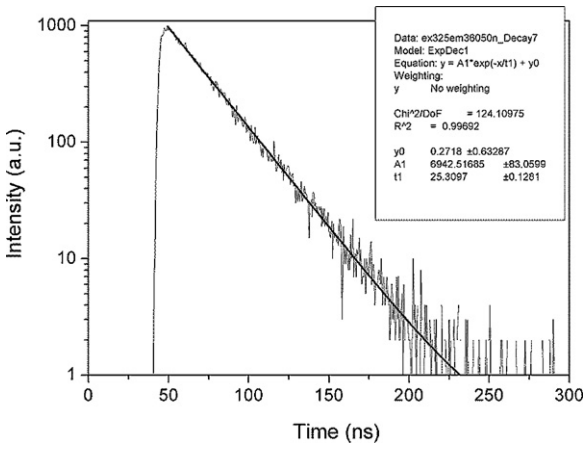

Fig. 7. Luminescence decay of 360 nm emission excited at 325 nm.

single crystals is still an unsolved problem. Manufacture of ceramic samples is a possible alternative way. For example, effectiveness of thin layers made from ground pyrosilicate crystals has been demonstrated at detection of thermal neutrons [27].

4. Conclusions

Crystalline samples of tetragonal gadolinium pyrosilicate (β-$Gd_2Si_2O_7$) are obtained for the first time. In contrast to other pyrosilicates, in β-$Gd_2Si_2O_7$ Gd^{3+} ions occupy four types of sites with different symmetry and coordination numbers. Consequently, in the case of RE doping, four types of emission centers can occur in this structure. This material shows the high yield of luminescence, nanosecond decay and, therefore, can be considered as promising scintillator material.

Acknowledgments

We acknowledge with thanks our colleagues from Institute for Scintillation Materials NASU, namely, Prof. V. Cherginets and Dr. T. Rebrova for consultancy on features of phase diagrams for rare-earth silicates, Dr. O. Vyagin for help in ceramic samples preparation, and S. Vasyukov for help in luminescence measurements.

References

[1] P. Lecoq, A. Annenkov, A. Gektin, M. Korzhik, C. Pedrini, Inorganic Scintillators for Detector Systems, Springer-Verlag, Berlin-Heidelberg, 2006.
[2] Y. Wu, D. Ding, S. Pan, F. Yang, G. Ren, J. Alloys Compd. 509 (2011) 366–371.
[3] H. Yokota, M. Yoshida, H. Ishibashi, T. Yano, H. Yamamoto, S. Kikkawa, J. Alloys Compd. 509 (2011) 800–804.
[4] M. Gu, L. Jia, X. Liu, S. Huang, B. Liu, C. Ni, J. Alloys Compd. 502 (2010) 190–194.
[5] L. Pidol, A. Kahn-Harari, B. Viana, B. Ferrand, P. Dorenbos, J.T.M. de Haas, C.W.E. van Eijk, E. Virey, J. Phys.: Condens. Matter 15 (2003) 2091–2102.
[6] S. Kawamura, J.H. Kaneko, J. Haruna, S. Saeki, F. Fujita, A. Homma, S. Nishiyama, S. Ueda, K. Kurashige, H. Ishibashi, M. Furusaka, IEEE Nuclear Sci. Symp. Conf. N24-178 (2007) 1365–1367.
[7] J. Haruna, J.H. Kaneko, M. Higuchi, S. Kawamura, S. Saeki, Y. Yagi, H. Ishibashi, F. Fujita, A. Homma, IEEE Nucl. Sci. Symp. Conf. N24-210 (2007) 1421–1425.
[8] O. Sidletskiy, V. Baumer, I. Gerasymov, B. Grinyov, K. Katrunov, N. Starzhinsky, O. Tarasenko, V. Tarasov, S. Tkachenko, O. Voloshina, O. Zelenskaya, Radiat. Meas. 45 (2010) 365–368.
[9] H. Feng, D. Ding, H. Li, S. Lu, S. Pan, X. Chen, G. Ren, J. Alloys Compd. 489 (2010) 645–649.
[10] M. Nikl, G. Ren, D. Ding, E. Mihokova, V. Jary, H. Feng, Chem. Phys. Lett. 493 (2010) 72–75.
[11] M. Nikl, A.M. Begnamini, V. Jary, D. Niznansky, E. Mihokova, Phys. Status Solidi RRL 3 (2009) 293–295.
[12] H. Ishibashi, A. Homma, M. Furusaka, Prog. Nucl. Sci. Technol. 1 (2011) 288–291.
[13] Z. Zhanga, Yu. Wanga, F. Zhanga, H. Cao, J. Alloys Compd. 509 (2011) 5023–5027.
[14] N.A. Toropov, F.Ya. Galahov, S.F. Konovalova, Izv. AN USSR, OHN 4 (1961) 539–541.
[15] S. Kawamura, J.H. Kaneko, M. Higuchi, T. Yamaguchi, J. Haruna, Y. Yagi, K. Susa, F. Fujita, A. Homma, S. Nishiyama, H. Ishibashi, K. Kurashige, M. Furusaka, IEEE Nucl. Sci. Symp. Conf. N30-138 (2006) 1160–1163.
[16] S. Saeki, J.H. Kaneko, M. Higuchi, S. Kawamura, J. Haruna, F. Fujita, A. Homma, S. Nishiyama, S. Ueda, K. Kurashige, H. Ishibashi, M. Furusaka, IEEE Nucl. Sci. Symp. Conf. N24-212 (2007) 1426–1428.
[17] N.A. Toropov, I.A. Bondar, A.N. Lazarev, Yu.N. Smolin, Rare-earth Silicates and Their Analogues, Nauka, Leningrad, 1971 (in Russian).
[18] S. Kawamura, M. Higuchi, J.H. Kaneko, S. Nishiyama, J. Haruna, S. Saeki, S. Ueda, K. Kurashige, H. Ishibashi, M. Furusaka, Cryst. Growth Des. 9 (3) (2009) 1469–1473.
[19] I. Gerasymov, O. Sidletskiy, S. Neicheva, B. Grinyov, V. Baumer, E. Galenin, K. Katrunov, S. Tkachenko, O. Voloshina, A. Zhukov, J. Cryst. Growth 318 (2011) 805–808.
[20] H.S. Tripathi, V.K. Sarin, Mater. Res. Bull. 42 (2007) 197–202.
[21] G.M. Sheldrick, SHELX97, Program for the Solution and Refinement of Crystal Structures, University of Göttingen, Germany, 1997.
[22] J. Rodriguez-Carvajal, T. Roisnel, Full Prof.98 and WinPLOTR: New Windows 95/NT Applications for Diffraction, Commission for Powder Diffraction, International Union of Crystallography, Newsletter No. 20 (May–August) Summer 1998.
[23] J. Felsche, Struct. Bond. 13 (1973) 99–197.
[24] T.C. Ozawa, S.J. Kang, J. Appl. Crystallogr. 37 (2004) 679–680.
[25] N.C. Webb, Acta Crystallogr. 21 (1966) 942–944.
[26] L. Kepinski, M. Wocyrz, M. Marchewka, J. Solid State Chem. 168 (1) (2002) 110–118.
[27] N.Z. Galunov, B.V. Grinyov, N.L. Karavaeva, I.V. Gerasymov, O.Ts. Sidletskiy, O.A. Tarasenko, IEEE Trans. Nucl. Sci. 58 (1) (2011) 339–346.